بسم الله الرحمن الرحيم

BACHELOR OF SCIENCE IN ELECTRICAL &

ELECTRONIC ENGINEERING

A THESIS ON

ELECTRICAL AND MAGNETIC TRANSPORT PROPERTIES OF IRON-BASED METALLIC GLASS (FINEMET)

By

Deen Muhammad (Student ID: 082439)

Hussain Muhammad Farabi (Student ID: 082455)

MD. JubaerAlam (Student ID: 082445)

Electrical and Electronic Engineering Department
Islamic University of Technology (IUT)
The Organization of Islamic Conference (OIC)
Gazipur -1704, Dhaka, Bangladesh
October, 2012

ELECTRICAL AND MAGNETIC TRANSPORT PROPERTIES OF IRON-BASED METALLIC GLASS (FINEMET)

A Thesis Presented to
the Academic Faculty

By

Deen Muhammad (Student ID: 082439)

Hussain Muhammad Farabi (Student ID: 082455)

MD. JubaerAlam (Student ID: 082445)

In Partial Fulfillment of Requirement for the Degree of Bachelor of Science in

Electrical & Electronic Engineering

Under the supervision of

....……

Dr. Md. FerozAlam Khan
Professor,Department of Physics,
Bangladesh University of Engineering and
Technology,
Dhaka-1000, Bangladeshand
Coordinator, Dhaka Materials Science Group,
Phone: 880 2 966 5650 (PABX),
FAX: 880 2 861 3026, 880 2 861 30.
Email: fakhan@phy.buet.ac.bd

Declaration

This is to certify that the project entitled "**ELECTRICAL AND MAGNETIC TRANSPORT PROPERTIES OF IRON-BASED METALLIC GLASS (FINEMET)"**is supervised by **Dr. Md.Feroz Alam Khan** in Islamic University of Technology (IUT). This project work has not been submitted anywhere for a degree or diploma.

……

Dr. Md. Feroz Alam Khan

Professor, Department of Physics,
Bangladesh University of Engineering and Technology,
Dhaka-1000, Bangladesh.

……

Dr. Md. Shahid Ullah

Professor and Head of the EEE Department,
Islamic University of Technology,
Gazipur-1704, Bangladesh.

Authors

……	……	……
Deen Muhammad	**Hussain Muhammad Farabi**	**Md. JubaerAlam**
Student ID: 082439	Student ID: 08255	Student ID: 082445

Dedicated To…

Our

Beloved Parents

Acknowledgement

In the name of Allah, the Most Gracious and the Most Merciful,

First and foremost we offer our sincerest gratitude to our supervisor, Professor Dr. Md. Feroz Alam Khan, who has supported us throughout our thesis with his patience and knowledge whilst allowing us the room to work in our own way. We attribute the level of our Bachelor degree to his encouragement and effort and without him this thesis, too, would not have been completed or written. His invaluable guidance, extensive knowledge and deep insights are what made this achievement possible. One simply could not wish for a better or friendlier supervisor.

We like to thank all of our friends for their kind co-operation and special thanks must go to Farhana Zaman Glory.

Finally, we want to dedicate the essence of our purest respect to our parents who have made our existences possible. It is not really we who reached here, but of course it is our kind parents who gave us hope and inspirations. The greatest pleasure to us is to think about them.

Abstract

Electrical and Magnetic transport properties of $Fe_{78}B_{10}Si_{12}$ (FINEMET) metallic ribbons prepared by standard melt-spinning technique have been investigated. $Fe_{78}B_{10}Si_{12}$ shows conventional anisotropic magneto resistance (MR) which is found to vary from 0 - 15% with the external magnetic field. An external transducer is used to vibrate the sample in an external magnetic field and to investigate the dynamic behavior of the sample. It is observed that a small self-induced ac voltage is super imposed on the dc response of the sample. This small ac signal is observed to be periodic in nature and may be attributed to the presence of non-magnetic metallic species in the ribbon. The effect of temperature (ranging from 30^o- 550^o) on the resistivity of the sample is measured and the glass transition temperature, T_g of the alloy is estimated from the dc resistivity anomaly observed at the elevated temperature. The frequency dependent response of impedance, phase angle, permeability, permittivity, Quality factor, Dissipation factor are also studied by Wayne Kerr Impedance Analyzer with frequency range of 100Hz-100MHz. The observed electrical and magnetic properties of the material indicate that the alloy in its ribbon form is suitable for its potential use in electrical and magnetic switching devices.

Keywords

FINEMET, Ferromagnetism, Magneto resistance, Self-Induction Resistivity, Impedance, Permittivity, Permeability, Quality Factor, Dissipation Factor.

List of Figures

Table of Contents

.

Preface

In the first chapter, we have introduce the subject by discussing different aspects of amorphous and BMG the Bulk Metallic Glass materials. The descriptions of different experimental techniques along with the experimental procedures followed in this work are elaborated in chapter 2. Our experimental results are discussed in chapter3. In chapter 4, the thesis work is summarized.

Chapter 1

Introduction

1.1 Amorphous, Glassy and Bulk Glassy Metals

An amorphous metal (also known metallic glass or glassy metal) is a solid metallic material, usually an alloy, with a disordered atomic-scale structure. Most metals are crystalline in their solid state, which means they have a highly ordered arrangement of atoms as shown in figure 1.1(a). Amorphous metals are non-crystalline, and thus are glasses as shown in figure 1.1(b). By definition, a glass is a solid material obtained from the liquid melt which retains the disordered structure during solidification. When this glass contains enough (50 to 80 at. %) metallic elements it is referred as metallic and its physical properties are significantly enhanced compared to those of a crystalline analogue of the same composition [1]. Unlike the usual glasses, such as window-glass, which are insulators, amorphous metals have good electrical conductivity.

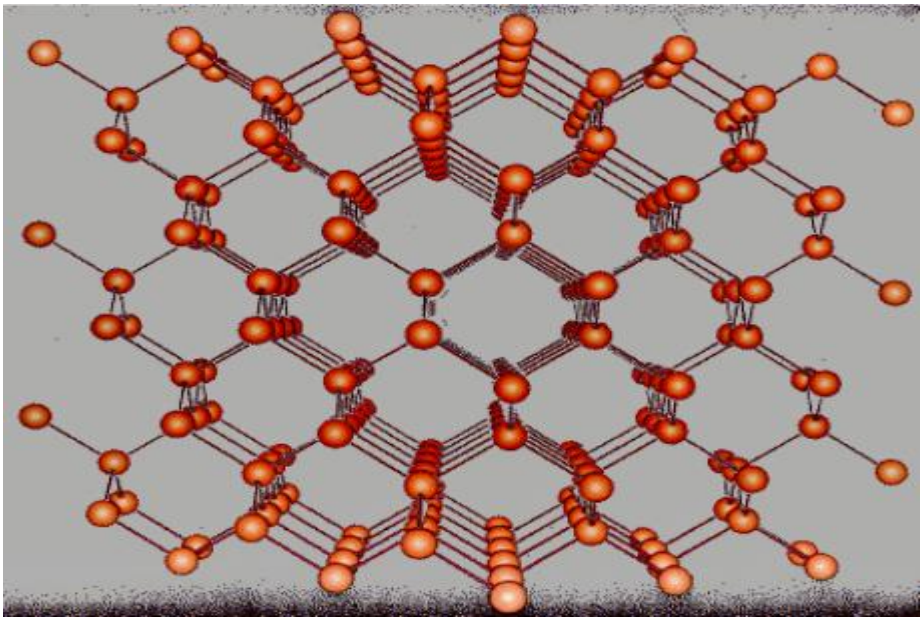

Figure 1.1(a): Crystalline structure of Metal

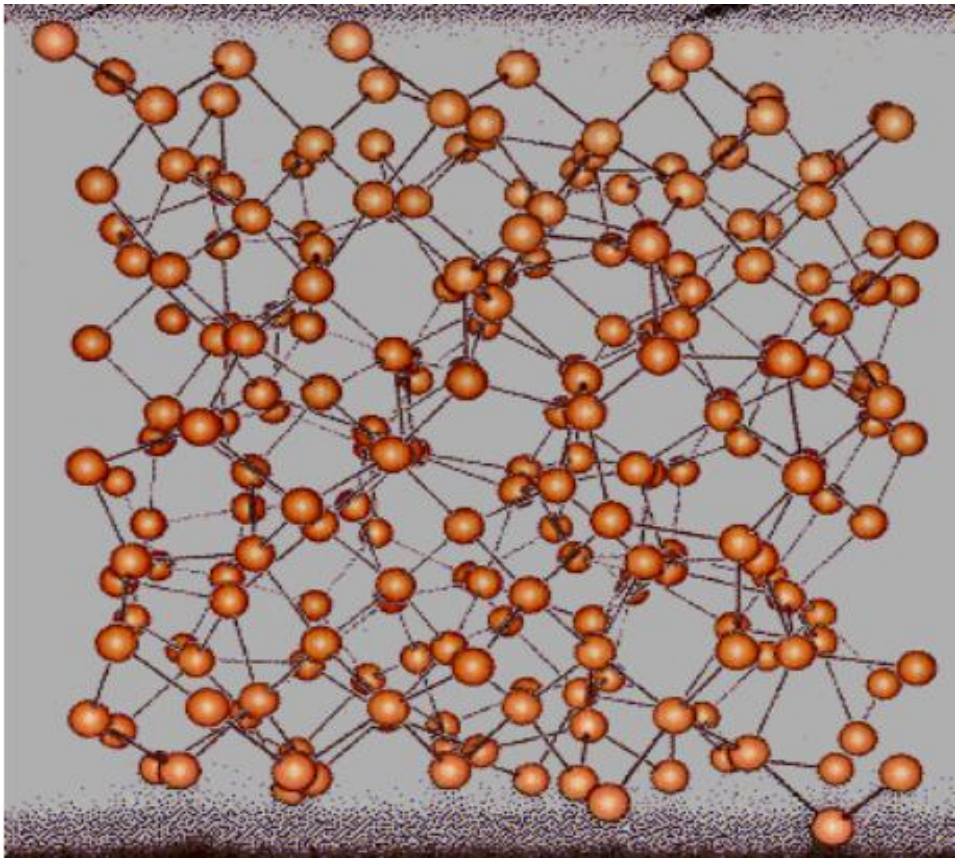

Figure 1.1(b): Non crystalline structure of metallic glass

The recent development of bulk metallic glasses (BMG's) has opened the door for use of these fascinating materials in structural applications. The amorphous alloys and Bulk Metallic Glassy alloys (BMG) may be distinguished on the basis of cooling rates and the thermal response as the material is heated above room temperature. The former needs very high cooling rate (~10^6 K/s) to be amorphized while the latter can be achieved at much low quench rates of 1-100 K/s. The amorphous alloys and BMG materials can be differentiated by observing their phase transformation on heating as shown in figure 1.2

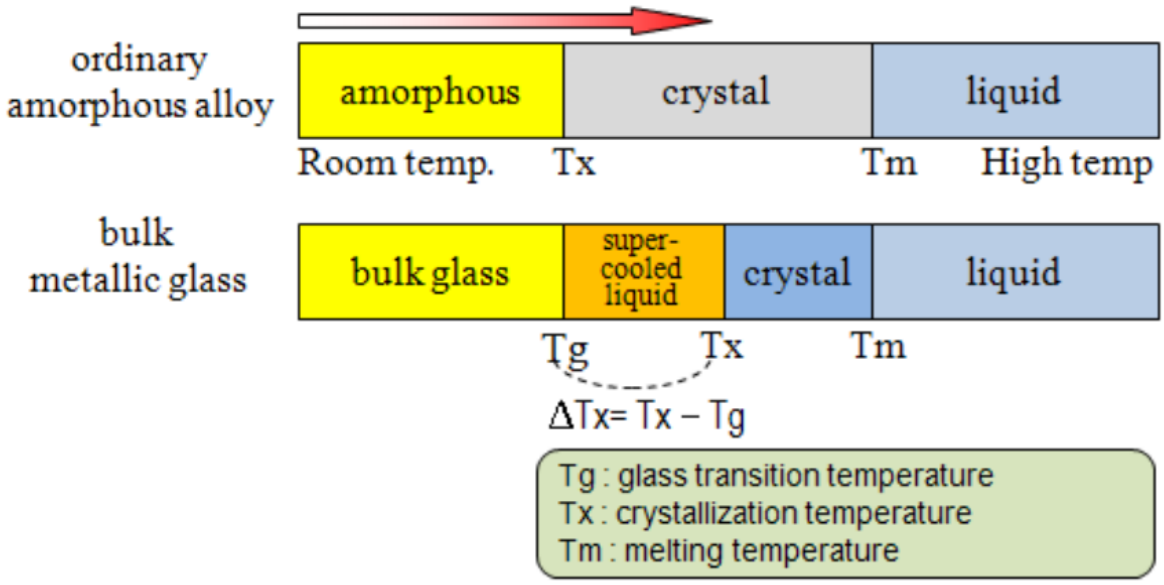

Figure 1.2: Transformation of amorphous and BMGs glasses on heating.

When an ordinary amorphous alloy is heated it passes through crystalline phase before attaining the liquid form. On the other hand, BMG traverses super cooled liquid region before crystallization and the liquid state. In short, the existence of super cooled liquid region is the major difference between amorphous and bulk glassy metals. On cooling appropriately from the super cooled regime the glassy state can be recovered, which is not possible with conventional amorphous alloys. Thus in a super cooled state the alloy can be molded into near net shapes while still maintaining the glassy state at room temperatures.

1.2 Brief History of Metallic Glass

The research in the field of metallic glasses started since the discovery of ability to amorphize $Au_{75}Si_{25}$ by Pol. Duwez in 1960 by means of a piston anvil technique [29]. During 1970 to 1980 once the ability to cast long ribbons was invented by H.S. Chen, there has been extensive research mainly in Japan and USA with active commitments by Allied Chemicals promoted on a commercial scale production of ribbons, and wires of literally thousands of metallic glasses of a variety of compositions. However, the high quenching rate limited the geometry of metallic glasses to ribbons and thin sheets. This barrier was broken by Turnbull [30, 31] and his coworker playing a key role to develop the bulk metallic glasses. Consequently, Chen in

1974 succeeded to prepare the first bulk metallic glass (BMG) of Pd-Cu-Si alloy with low cooling rate of 10^3K/s by using the suction casting method [32]. Later on Turnbull and coworkers reported Pd-Ni-P BMG with 10 mm thickness by using boron oxide fluxing method [33, 34]. For a long period before 1990, due to the necessity of high cooling rates (10^5 K/s) no BMGs have been synthesized except Pd-Ni-P and Pt-Ni-P systems.

In early 1990s, Inoue et al. succeeded in producing new multicomponent BMG systems with cooling rates as low as (100 K/s), in a variety of combination of common metallic elements [35, 36]. They synthesized Zr, La and Mg alloy based BMGs by stabilizing super cooled liquids [37, 38, 39]. To develop BMGs for industrial applications as well as for scientific research purposes unrelenting efforts were put forth. Because of the excellent properties [40, 41] of early transition metal (ETM) (Zr, Ti, Lanthanide based, noble metal (Pd, Pt based systems) much attention was paid for their development. In such multicomponent BMG systems rods with maximum diameters of 30 nm for Zr-Al-TM (TM= transition metal) [42] and 40 to 72 mm for Pd-Cu-Ni-P were reported [43, 44]. On the other hands, due to high cost and unavailability of high purity raw materials of ETM based BMGs attention was drawn to fabricate late transition metal (LTM) such as Fe, Co, Ni and Cu based BMGs [45].

The first Fe based BMG (containing more than 50 at% LTM) was synthesized by A. Inoue in 1995 [46]. They categorized LTM based BMG system in two major parts. The metal group system consisted of Cu and Ni based alloys. While Fe, Co, Pt and Pd based alloys form metal metalloid group. For engineering applications, the metal BMGs have greater uses as compared to metal metalloid BMGs due to the simplified compositions. However, their glass forming abilities are lower than metal metalloid BMGs [36]. Another category of ternary and pseudo ternary glass forming systems is classified in group of five. The first group is composed of LTM, simple metal, and ETM e.g. Cu-Zr-Al. The second group consistsof LTM (Fe), metalloid (B, Si) and ETM (Nb). Third group includes LTM, (Al or Ga) metalloid system. Group four is indicated by ETMLTMTi systems and group five has LTM and Metalloid elements. The LTM based BMGs have excellent features such as the highest glass forming ability (GFA), larger temperature interval of super cooled liquid ($\Delta Tx = TgTx$) and reduced glass transition temperature (Tg/Tl) 36].

1.3 Mechanical properties of Iron-based Metallic Glasses

In the family of bulk metallic glasses (BMGs), Fe-based systems exhibit impressive mechanical properties including very high compressive strengths and very high hardness values [9]. Besides, they show good corrosion and wear resistance, and some of them exhibit good magnetic properties. Their attraction comes also both from the relatively low cost of their production and from their exceptional glass forming ability, allowing to cast rods with diameters above 1 cm for some of them [10]. Peculiar compositions include carbon atoms in sufficient content to name them amorphous steels [11]. However, all these materials are extremely brittle in tension, have poor toughness [12] and are brittle or quasi-brittle in compression [13]. This can compromise their use for potential engineering applications.

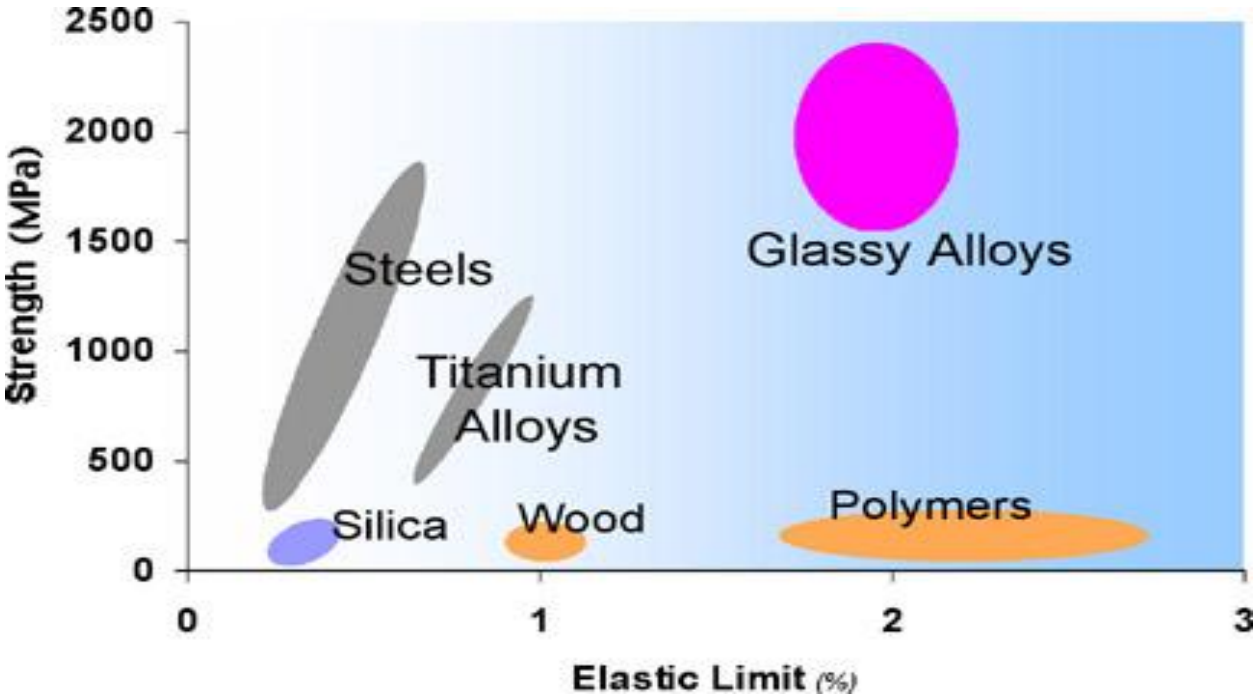

Figure 1.3: The strength (MPa) vs. Elastic limit (%) of glassy alloys in comparison with other materials

Iron-based BMGs exhibite fracture strengths near 4 GPa, 2–3 times those of conventional high-strength steels. The non-ferromagnetic amorphous steel alloys have glass-forming ability high enough to form single-phase glassy rods withdiameter

sreaching 16 mm [14]. In view of a recently observed correlation that exists between plasticity and Poisson's ratio for BMGs, compositional effects on plasticity and elastic properties in amorphous steels were investigated. For the new amorphous steels, fracture strengths as high as 4.4 GPa and plastic strains reaching ~0.8% were measured. Plastic failure instead of brittle failure was observed as the Poisson's ratio approached 0.32 from below.

The review paper by Payer et al. illustrates that many, but not all, amorphous metals exhibit superior corrosion performance in comparison to their crystalline counter-parts. Their extremely high strength provides the possi-bility of significant environmental effects on mechanical behavior, although relatively little work has focused on the general area of environmental effects on fracture of these emerging materials systems.

Alloy systhesis and mechanical testing

The effects of changes in stress state and alloy chemistry on mechanical behavior were investigated in a series of papers. Early experimental work by Chen [15] in-dicated that changes to the elastic constants (e.g., Poisson's ratio) of amorphous materials could control the magnitude of hardness and extent of deformation possible. More recent work by Johnson et al.[16] has suggested that high compressive ductility is similarly facilitated in metallic glasses with high Poisson's ratio.

1.4 Magnetic Properties of Metallic Glasses

1.4.1 What is Ferromagnetism?

Permanent magnetism is an atomic effect due to electron spin. In atoms with two or more electrons if they are usually arranged in pairs with their spins oppositely aligned are known as non-magnetic. And if the spin does not pain, that's the ferromagnetic case.

In ferromagnetic materials, negative exchange interactions between the intrinsic spins of neighboring magnetic atoms are favored when a parallel alignment of magnetic moments in neighboring atoms takes place. All ferromagnetic materials have a critical temperature above which it becomes paramagnetic due to thermal agitation. This temperature is called as Curie temperature (Tc) [4]. According to Weiss assumption the molecular field acted in a ferromagnetic substance below and above

its Tc, is so strong that it can magnetize the substance to saturation even in the absence of magnetic field. The substance is self-saturating or spontaneously magnetized [4].

Below Curie temperature, a piece of ferromagnetic material may not be spontaneously magnetized. The material is considered to be demagnetized that is its net magnetic moment is zero. A ferromagnetic material in the demagnetized state is divided into small regions known as magnetic domains or Weiss domains [4]. There remains a boundary wall called 'Domain wall' that separates two domains. Each domain encompasses a large number of atoms and is spontaneously magnetized to saturation value MS [5]. From one domain to the other, the direction of magnetization of different domains varies in such a way that the net magnetization of the whole sample is zero. The magnetization process is then to convert the specimen from multi domains into a single one at which the whole sample is a single domain magnetized in the direction of applied field [4]. The distribution of domains and its consequence on the effective magnetization in an applied magnetic field gives rise to initial magnetization curve as shown in the figure 1.4(a),1.4(b).

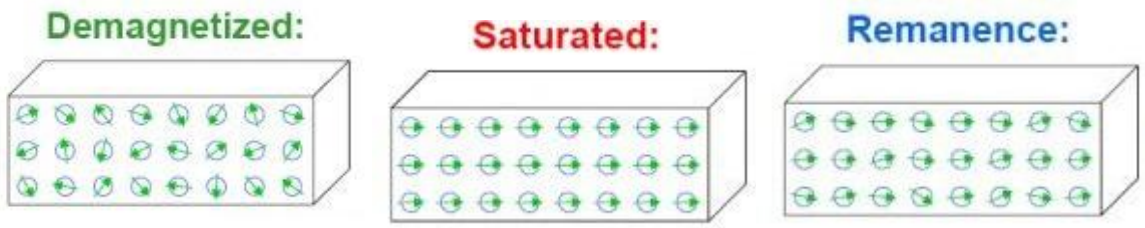

Figure 1.4(a): Convenient domain structure of ferromagnetic materials.

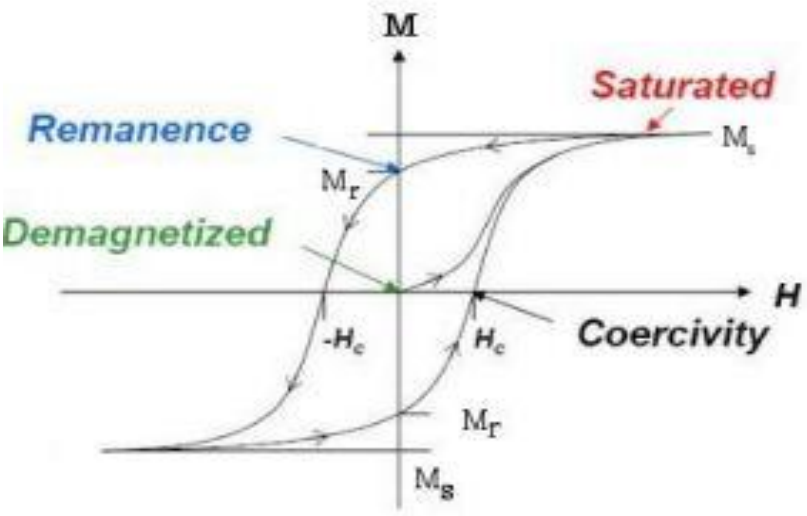

Here, $B = \mu_o (H + M) = \mu_o H + J$

Figure 1.4(b): Convenient hysteresis loop for ferromagnetic materials.

So at macroscopic level, the field induces magnetization that saturates in a ferromagnetic material [5] if the applied field is large enough. However, the magnetization process is reversible if the applied field is continuously varied between two extreme values +H0, -H0 [5]. This describes the hysteresis loop. The initial magnetization curve, hysteresis loop and saturation magnetization are characteristics of ferromagnetic materials [5].

1.4.2 Types of Ferromagnetic materials

Ferromagnetic materials can be classified as:

Soft magnetic materials:

If migration of domain wall can happen easily then the ferromagnetic material will be saturated at low magnetic field. Such ferromagnetic materials are considered as soft magnetic materials [6].

Characteristics:

1. High saturation magnetism
2. Low magneto crystalline anisotropy
3. Low coercive field
4. High Curie temperature
5. High electrical resistance

Hard magnetic materials:

If the migration of domain wall is difficult the ferromagnetic material can only be magnetized by applying high magnetic field. But once the material is magnetized and its demagnetization is difficult then such ferromagnetic materials are known as hard magnetic materials [6].

Characteristics:

1. High magnetic response
2. Easy and fast attain of saturation
3. Easy magnetic domain wall movement (homogeneous material without defects, inclusions, stress etc.)
4. Magnetic stability at higher temperature
5. Minimum magnetic losses due to magnetic currents.

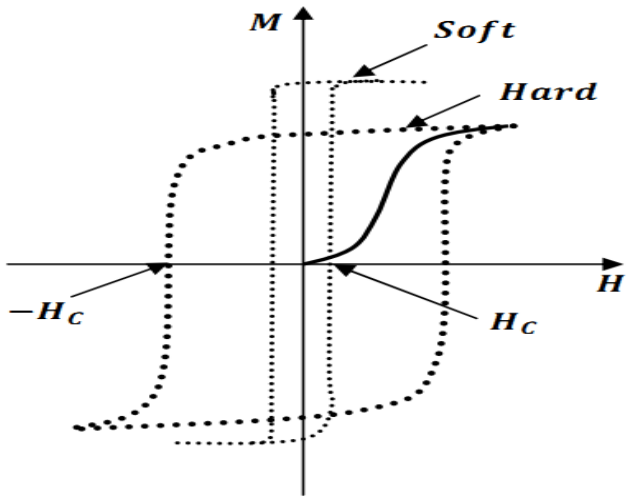

Figure 1.5: Typical hysteresis loop for soft and hard magnetic materials

1.4.3 Phenomena of Ferromagnetism in metallic glasses

The ferromagnetism is not only confined with crystalline alloys but also with metallic glasses except that in metallic glass since the structural disorder is the same in all directions the material is magnetically isotropic. The first strongly ferromagnetic metallic glass of $Fe_{70}P_{15}C_{10}$ with Curie temperature around 320° C, magnetic moment per Fe atom 2.10±0.01 $\mu_B$as compare to pure crystalline Fe (2.22 μ_B)and coercivity 3 Oe became the prototype for all ferromagnetic metallic glasses till date. However, the magnetic behavior depends upon, the field annealing the alloy composition (in our case it is $Fe_{78}B_{10}Si_{12}$) and the induced anisotropy during solidification.

The internal stresses produced by liquid quenching may introduce magnetic anisotropy in metallic glasses. It has been observed that these internal stresses can be drastically reduced by appropriate heat treatment [1]. The magnetic properties of metallic glasses when compared with that of crystalline alloys reveal that metallic glasses have a lower Tc value (The phenomena occurs due to the reduced proportionate to the concentration of glass former), high permeability, low coercivity. Also the electrical resistivity will contain a large disorder contribution in it. For instance, Metglass 2605 SC(Fe81B13SI3.5C2) compared with that of crystalline steel Fe3Si shows that saturation induction of metallic glass is lower to about 81% (1.80T) than that of crystalline Fe (2.1T) [2,3].

1.4.4 Comparison of soft magnetic properties between thin ribbons & Bulk magnetic glasses

In comparing glassy thin ribbons and BMGs (Bulk Metallic Glasses) it has been observed that Fe and Co based BMGs exhibit advantageous soft magnetic properties than the metallic glassy ribbons [7]. The specific differences are: [8]

1. At room temperature electrical resistivity is high (200-250 μΩ-cm)
2. Permeability at initial stage is also very high
3. Coercive field is low (0.2-4 A/m)
4. Domain wall structures are controlled.

Though BMGs are of Fe, Co and Ni based but among these Fe-based materials are most popular because of their good magnetic properties (i.e. high saturation magnetization, very low coercivityetc). But one problem is that Iron-based materials have low GFA (Glass Forming Ability). But recently a lot of research works are going on in order to improve their GFA to fabricate BMAs in a large extend.

1.5 Electrical Transport properties of Metallic Glasses

The study of the electrical transport properties of amorphus metallic alloys has unearthed many new phenomena and has necessitated a paradigm shift to explain the contrast between crystalline and amorphus metallic systems.

In transport properties, electrical resistivity is a very sensitive tool for analyzing the different scattering processes which happen in the metallic system. Resistivity is sensitive to various metallurgical factors such as disorder, structural relaxation [17], variation in local atomic arrangements [18], size effect (free volume differences in ribbons because of rapid quenching speed difference) etc.

For analyzing this property we need to concentrate on two factors:

1. The resistivity is of the order of 100 μΩ-cm at room temperature which is roughly two orders of magnitude larger than it is for the crystalline analogue and
2. Secondly they have very small Temperature co-efficient of resistance (TCR). This value is in the range of $\pm 10^{-4} K^{-1}$ [1].

The high disorder residual resistivity at 0 K [1] are responsible for these . The reason for this high value of resistivity is the increase in scattering of conduction electrons due to temperature independent random atomic arrangement. The small value of TCR is related to the temperature dependence of the structure factor characterizing an amorphous material . In many metallic glasses depending on the relative position of the Fermi vector with respect to the maximum in the structure factor the TCR it can be positive or negative which can be brought about by the change of composition of the alloy. Furthermore, the general features for the resistivity of amorphous transition metals can be summarized as follows:

- They show a larger residual resistivity (ρ_0) than in the crystalline phase arising from the high disorder in the materials, and are comparable with corresponding liquid alloys.
- If ρ_0<150μΩ-cm, TCR is small and positive and it is negative with ρ_0>150μΩ-cm. Thieserelations seem to be valid in most of the disordered transition metal alloys.

Electrical resistivity with high value and small TCR might be of interest for designing measuring instruments in which the electrical circuits may need resistive components insensitive to temperature [1].

Chapter 2

Experimental Methods

2.1 Fabrication Techniques

Amorphous alloys can be prepared by a number of techniques. The basic procedure is to rapidly quench the metallic system either from its vapour phase or liquid phase on a heat sink so as to bypass the crystallization quickly to produce non crystalline structure akin to frozen liquid. These techniques are broadly classified into two categories:

1. Melt-quenching and
2. Deposition techniques.

Melt-quenching method includes:

- Splat-cooling,
- Roller-quenching,
- Spark erosion and
- Laser glazing [19-21]

Fabrication of amorphous alloys in a concentration range away from the eutectic point is facilitated by the deposition techniques which include vacuum thermal evaporation [22] and sputter deposition [23]. Other occasionally used techniques are electro deposition [24], ion-implantation [25] and solid-state diffusion [26].

2.1.1 Splat Quenching

This is the easiest and simplest form of Melt-quenching method. In this method, a liquid alloy droplet is squeezed between a rapidly moving piston and a fixed anvil alloys obtained by this method are in the form of thin discs (1-3 cm in diameter and20-60 µm in thickness).

2.1.2 Laser Quenching

Laser quenching [28] is another form of melt quenching technique. In this method, a short and highly intense laser beam is used to melt a portion of a thin metallic surface, which is then cooled rapidly by the surrounding crystal. The cooling rates achieved in this way are in the range of 10^{10} to 10^{12} K/s.

2.1.3 Melt-spinning

Melt spinning is the commonly employed versatile technique to fabricate thin ribbons which was conceived by Pond and Maddin (1969) [29]. Then later, Leibermann and Graham [30] used it as a continuous casting technique. This method employs a jet from which alloy melt is dropped onto a rapidly moving wheel made of a material with high thermal conductivity such as copper, shown in Fig 2.1

Continuous ribbons of amorphous alloys are obtained by this method and higher cooling rates (10^6 K/s) are achieved compared to splat-quenching.

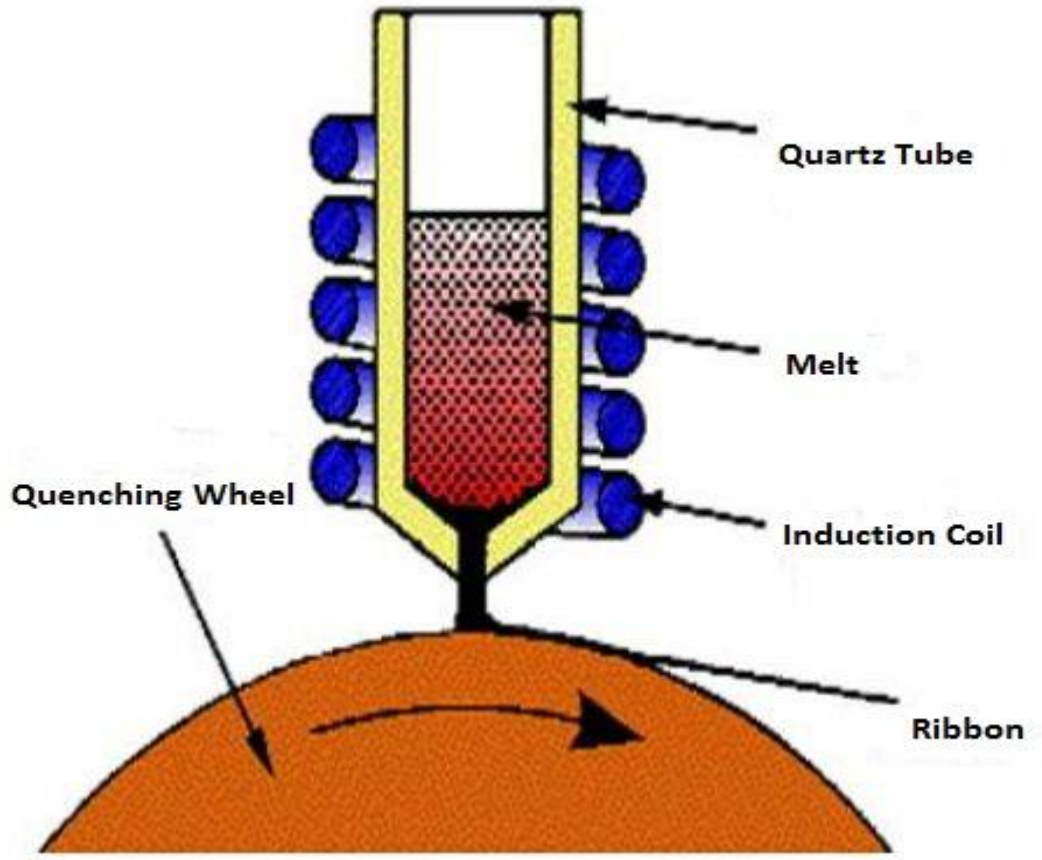

Fig 2.1: Schematic diagram of single roller quenching technique.

2.1.4 Copper Mold Casting

The casting technique has the same airtight chamber as in melt spinning method, along with quartz tube surrounded by induction coil. The only difference is the replacement of copper wheel with copper mold.

Fig 2.2: Copper mold tubes

For the fabrication of BMG rods, the molten alloy is injected into a selected mold of few mm diameters, by using the argon overpressure. Through this technique one may achieve the cooling rate of 10^2 K/s.

2.2 Characterization Techniques

2.2.1 X-Ray Diffraction

X-ray diffraction (XRD) is a versatile and non-destructive analytical technique to determine phases, orientation and to identify the structural properties of the crystal.

XRD patterns can only be observed when the size of obstacle is comparable to the wavelength of the electrons. Electrons and neutrons have wavelengths (say x-ray) comparable to atomic dimensions. When the monochromatic beam of x-ray is incident on the specimen and reflected from different planes, the interference take place

between x-rays reflected from adjacent planes. According to Bragg's Law, constructive interference can only occur among the reflected beams of x-rays from regular planes of atoms when the difference in path length is equal to an integral number of wavelengths. Mathematically,

$$2d\sin\theta=n\lambda$$

Where, d=inter planer distance

θ=Bragg angle

λ=an integer

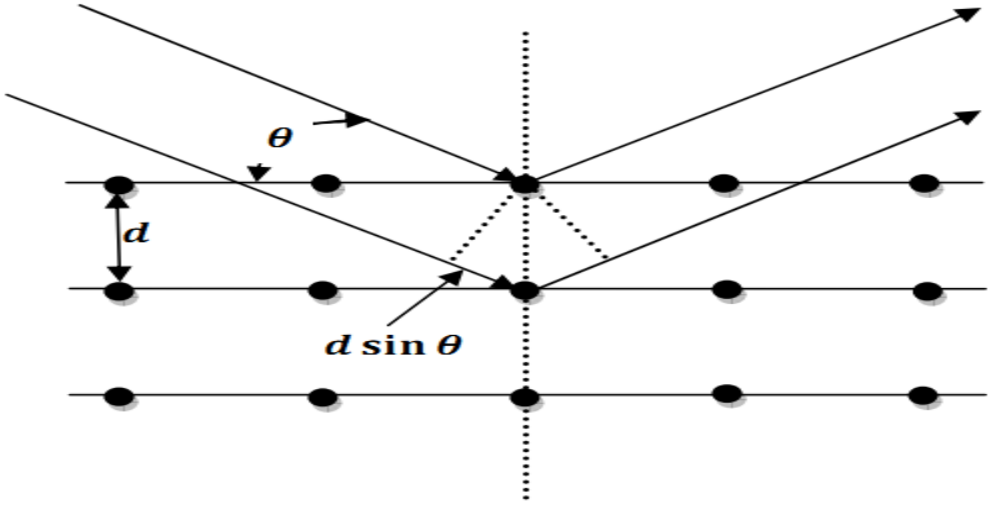

2.2.2 Vibrating Sample Magnetometer

A vibrating sample magnetometer (VSM) devised by S. Foner is a standard and effective technique for measuring magnetic material properties such as; saturation magnetization, coercivity, hysteresis and anisotropy. The working principles of VSM is based on Faraday Law of Induction that is by changing magnetic field an induced electromotive force (emf) is generated.

VSM operation starts by simply vibrating a magnetic sample along the zaxis normal the external DC magnetic field between pickup coils. So the sample is magnetized by the magnetic field. A magnetic field around the sample will be created by the magnetic

dipole moment of the sample and is known as Magnetic Stray Field. The variations in the stray field occurring when the sample is vibrating along z axis due to the sample movement are sensed by the pick-up coils.

According to Faraday Law, the oscillatory motion of the magnetic sample causes induced emf in the pick-up coils. This induced voltage is proportional to the sample's magnetization. A lock in amplifier is used to tune and amplify this induced current at the frequency of operation. All the components are attached with computer interface from where we can obtain the measurements. In our present case, the investigation of magnetic properties of all samples was performed by using home-made vibrating sample magnetometer (VSM) at room temperature.

Figure 2.3: VSM setup in the lab

2.2.3 Wayne Kerr Impedance Analyzer

To find the dependency of different parameters such as impedance, phase angle, permeability, permittivity, Quality factor, Dissipation factor on frequency we used Wayne Kerr Impedance Analyzer as shown in figure 2.4. The frequency range was 100Hz to 100 MHz. Toroidal shaped sample was used to get the necessary curves.

Figure 2.4:Wayne Kerr Impedance Analyzer

2.2.4 Four Point Probe Technique

In this thesis work four point probe technique was used to measure the resistivity and magneto-resistance of the ribbons. The schematic four point probe configuration is shown in the figure 2.5

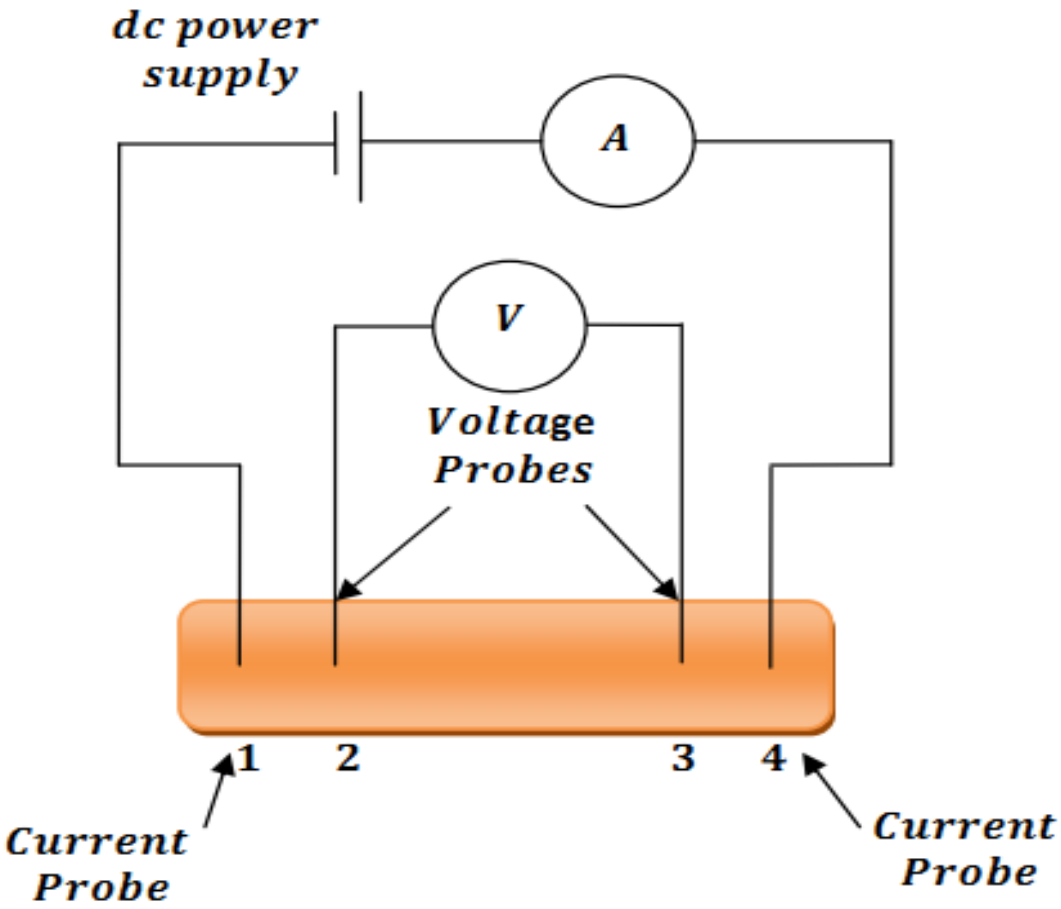

Figure 2.5: A schematic of Four Point Probe configuration

A four point probe has equally spaced four metal tips. To avoid the sample damage during the probing, one side of each probe is supported by a spring. The outer two probes (1&4) are used for current supply and inner two (2&3) for voltage measurement.

The resistance of the sample was determined by simply using the Ohm's law relation

$$R = V/I$$

Where the V is the potential and I is the current passing through the two electrodes.

By calculating the cross sectional area (A) of our samples and the length (L) between two electrodes we calculated the resistivity (ρ) with relation

$$\rho = R*A/ l$$

In the thesis work the I-V characteristics of all quenched samples were studied and then resistance (resistivity) was calculated from the slope of linear I-V curve.

Chapter 3

Experimental Results and Discussion

3.1 X-Ray Diffraction Patterns

The X-Ray diffraction pattern of our sample ($Fe_{78}B_{10}Si_{12}$) is shown in figure 3.1. The initial broad peak in the Intensity versus 2Θ curve at low angle of diffraction confirms the amorphous nature of the material. In case of crystalline, we rather see more spiked curve.

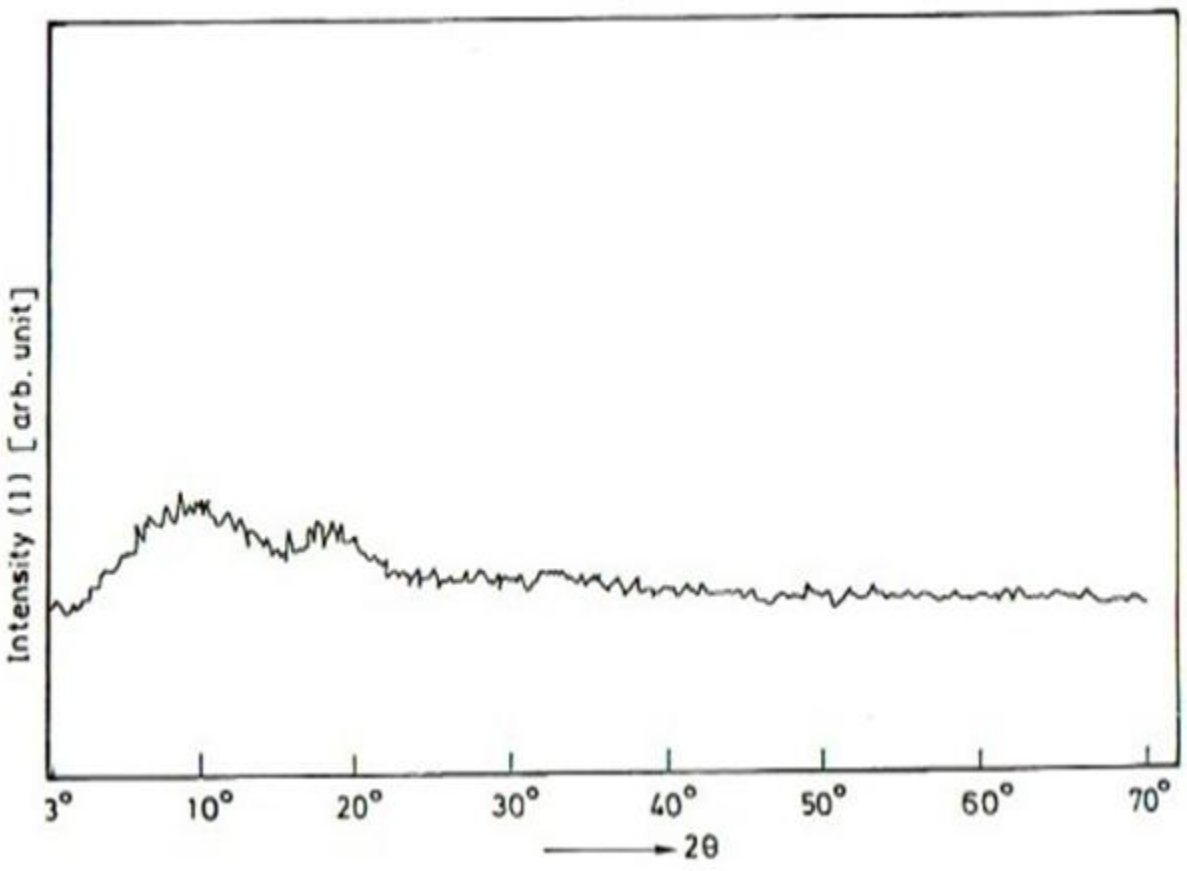

Figure 3.1 :X-Ray diffraction pattern of $Fe_{78}B_{10}Si_{12}$

3.2 Measurement of Electrical Resistivity(ρ)

Using 4 probe technique as stated earlier current was varied across the sample ranging from 0.1A to 2.0A at an interval of 0.1 A and corresponding voltage across the sample was measured. The data were plotted to get the I-V characteristic of the Sample as shown in the figure 3.1. From the I-V characteristic, resistance of the sample was measured by using simple Ohms Law of R=V/I and hence the electrical (ρ) of the sample was calculated.

.

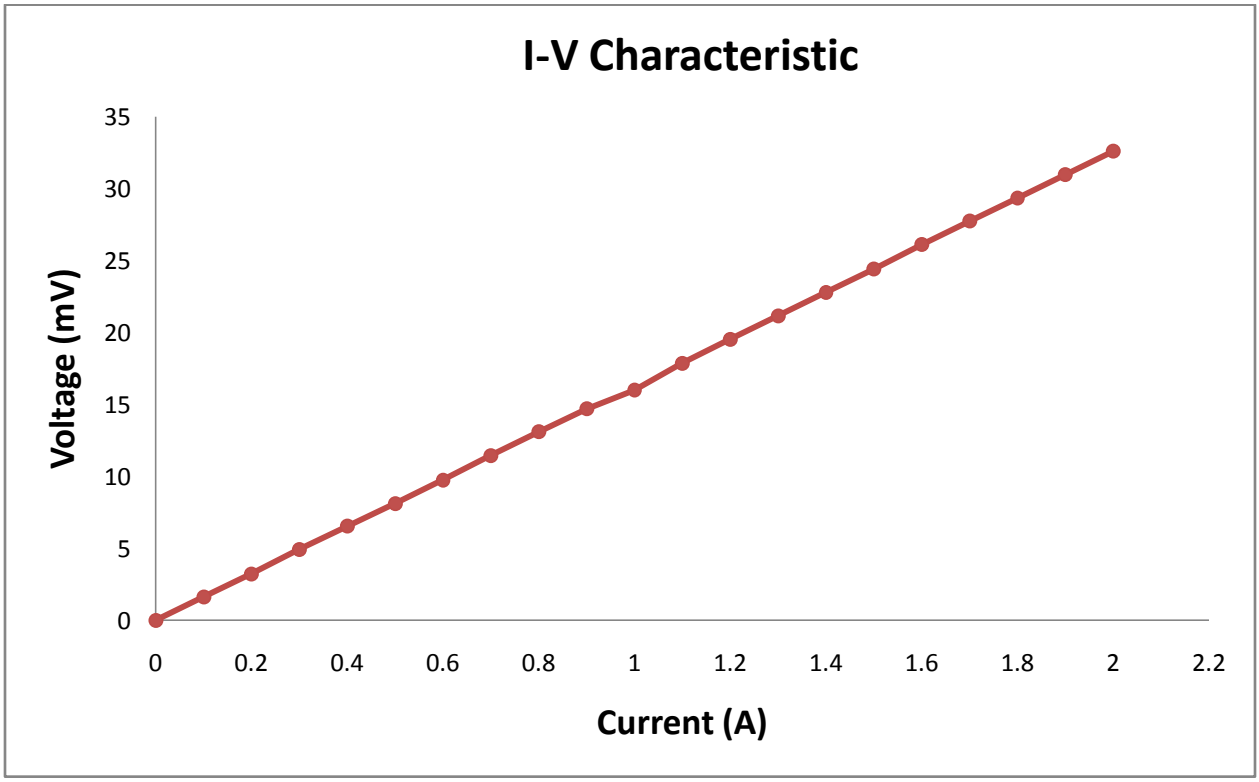

Figure 3.2: I-V characteristic of the sample

Calculation:

Resistance measured = 16.3mΩ

Thickness of the sample = 20µm

Width of the sample = 4.2mm

Area of cross-section , A =width*Thickness=84*10-9 m^2

Length of the sample, l = 16.065 mm

Resistivity ,ρ = R*A/ l = 1.27*10^{-6}Ωm

3.3 Field dependent Magneto Resistance:

Magneto resistance, where the resistance of the material changes with applied magnetic field, occurs in all metals. Classically, the MR effect depends on both the strength of the magnetic field and the relative direction of the magnetic field with respect to the current. The net effect is that the electrical resistance has maximum value when the direction of current is parallel to the applied magnetic field and has minimum value when the direction of current is perpendicular to the applied magnetic field. In our case we applied a magnetic field perpendicular with the direction of the current and measured the corresponding change in the resistance of the sample. Same 4 probe technique was applied for the experiment and I-V characteristic of the sample was measured for different magnetic field ranging from 1KG to 8KG and plotted as shown in the figure 3.2.

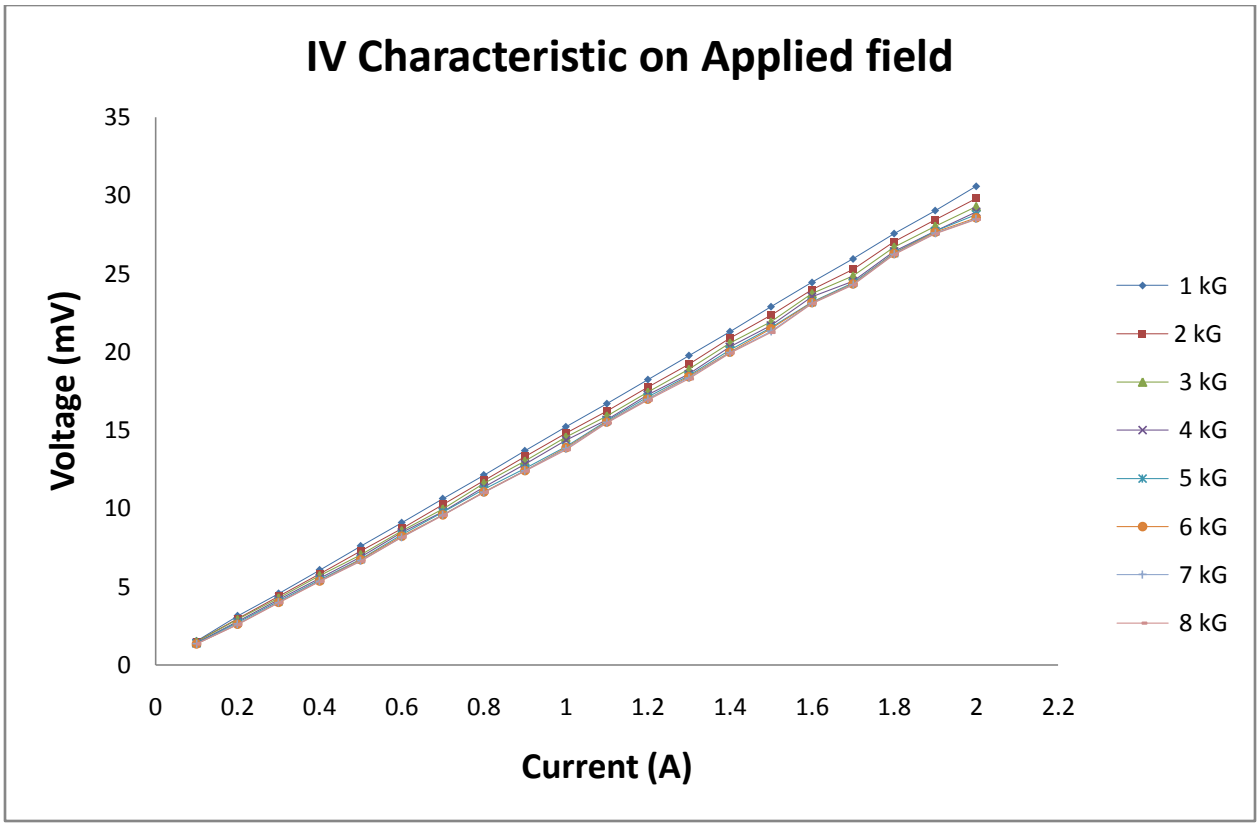

Figure 3.3: IV Characteristic of the sample on different Applied field

Calculation:

Magnetic Resistance,

$$MR = (R_0 - R_h)/R_0 \times 100\%$$

Where,

R_h = Resistance of the sample on corresponding applied magnetic field

R_o = Resistance of the sample without applied magnetic field

= 16.3 mΩ (measured earlier)

Measured MRs in different magnetic fields calculated are shown in figure 3.3.

Applied Magnetic Field	Corresponding Resistance(R_h)	Corresponding MR(%)
1KG	15.2578	6.3934
2KG	14.8013	9.194
3KG	14.4931	11.0849
4KG	14.2397	12.6396
5KG	14.0484	13.8131
6KG	13.9434	14.4571
7KG	13.8905	14.7821
8KG	13.8476	15.0451

Figure 3.4: Measurement of MR (%) on different applied field

So resistance of the sample is actually decreased as expected as the applied magnetic field is perpendicular with the direction of the current. Now we plotted magneto resistance (MR%) with respect to applied magnetic field as shown in figure 3.4.

From the curve we can see that the resistance of the sample can be varied within a range of 0-15% by applying external magnetic field. As we increase the value of the applied magnetic field greater than 8KG the changes in Magneto Resistance (MR%) is tends to zero.

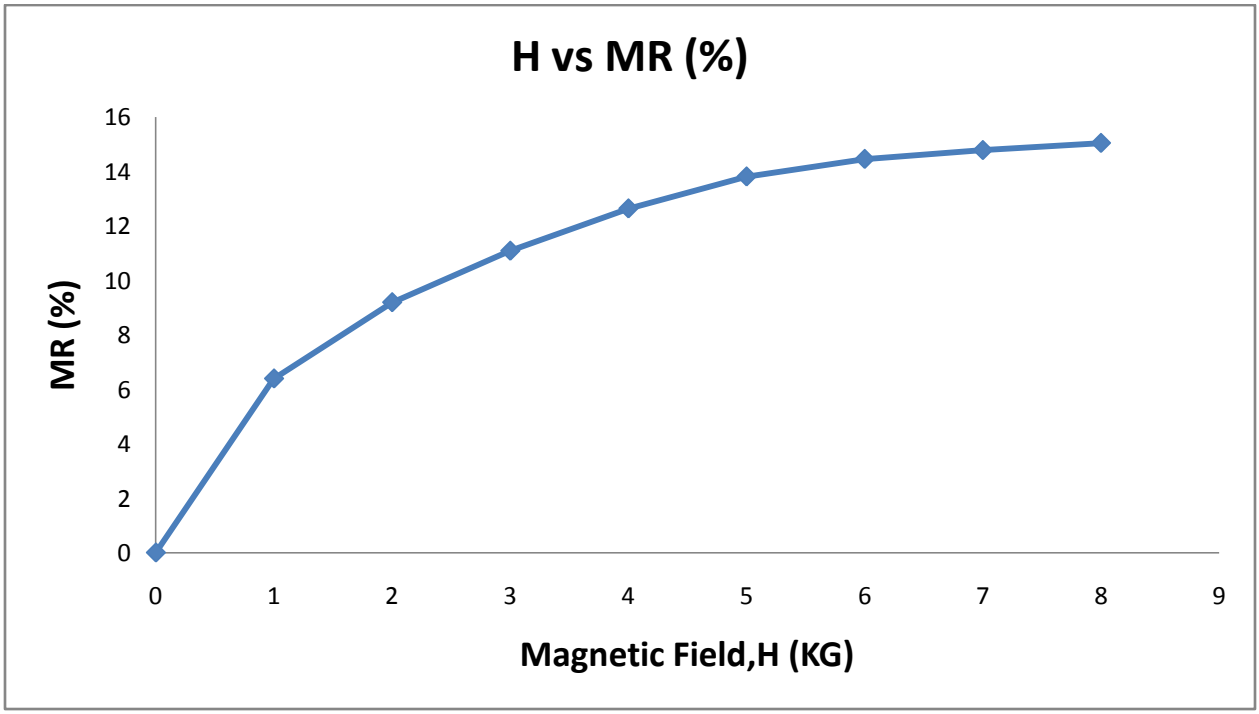

Figure 3.4 : Magnetic field vs Magneto Resistance(MR%)

3.4 Self -Induction due to external transducer

The property of self-inductance is a particular form of electromagnetic induction. Self-inductance is defined as the induction of a voltage in a current-carrying wire when the current in the wire itself is changing. In the case of self-inductance, the magnetic field created by a changing current in the circuit itself induces a voltage in the same circuit. Therefore, the voltage is self-induced. This effect derives from two fundamental observations of physics: First, that a steady current creates a steady magnetic field and second, that a time-varying magnetic field induces a voltage in a nearby conductor (Faraday's law of induction). From Lenz's law, a changing electric current through a circuit that has inductance induces a proportional voltage which opposes the change in current (self-inductance). The time varying field in this circuit may also induce an e.m.f. in a neighbouring circuit (mutual inductance).

In our case the sample was placed between the two magnetic poles and with the help of a external transducer it was vibrated with a frequency of 37Hz. It is anticipated that an eddy voltage would be created in the Material Under Test (MUT) due to the presence of some trace elements of metallic ions in the MUT. This induced eddy current which will produce an opposing magnetic field to the external field is also time-varying and will have a frequency of the transducer driver. The idea was to investigate whether this eddy response could be measured in this particular case. A 4 probe technique was used to measure the corresponding I(dc)-V(ac) (superimposed on the dc resistance) for different values of magnetic field varying from 1KG to 8KG and the corresponding curves are plotted and shown in figure 3.5.

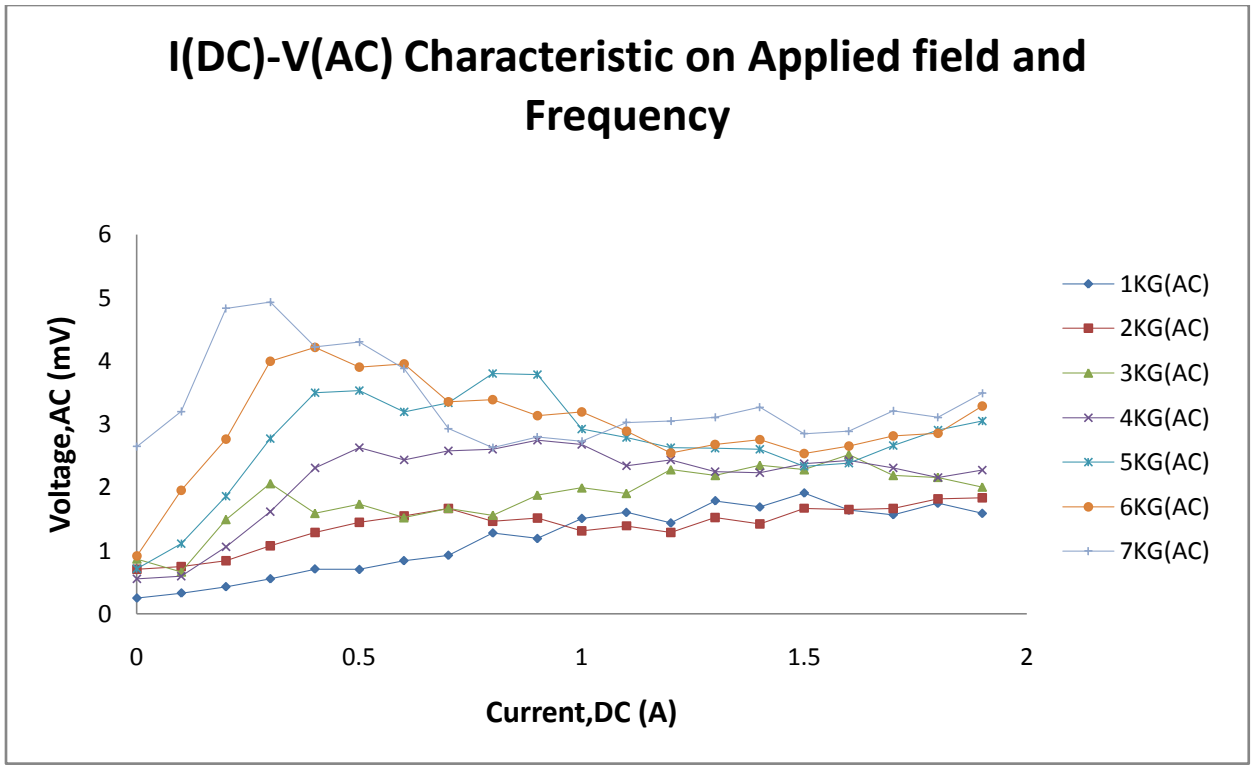

Figure 3.5:I(DC)-V(AC) Characteristic on Applied field and Frequency

The sample (MUT) vibrates with a frequency of 37 Hz and it cuts the magnetic flux periodically (37Hz.) creating an eddy current inside the MUT. It is observed that a small eddy voltage is super imposed on the dc response of the sample. This small ac signal is observed to be periodic in nature and may be attributed to the presence of non-magnetic metallic species in the ribbon. We did not get the oscillating voltage at lower current (Low magnetic field) because at low field the Eddy Voltage is so weak that the external dc magnetic field simply over rides the low Eddy voltage.

3.5 Resistivity Dependency on Temperature

Depending on temperature the electrical resistivity shows a series of anomalies, especially around temperatures where first or second range transitions take place. At low temperatures the electrical resistivity should tend to zero, but due to the structure defects and impurities, it tends to a constant value, bypassing the linear dependence. If the impurities presented in a certain metal have an electronic spin, then the electrical resistivity shows a minimum or a maximum characteristic. This behaviour is known as Kondo effect. Rein et al have studied the electrical resistivity of some alloys of Metglass

type under temperatures variation between 1.5 and 800 K as well as the influence of the crystallization on the electrical resistivity. The authors have noticed a minimum value of electrical resistivity in the case of the above mentioned alloys. It was also noticed that between the temperature of ρ_{min} and the Curie temperature there is not any correlation. The electrical resistivity of the amorphous and crystalline phases in the vicinity of T_{cr} (critical temperature) is relatively low. That means the basic contribution to the modification of the electrical resistivity is introduced through the chemical disorder and not through the material structure. In the case of Metglass alloys it was also noticed that the crystallization causes the further modification of the minimum electrical resistivity.

In our experiment the changes of resistivity was measured by increasing the temperature ranging from 30-550 °C and after plotting the data we get the curve as shown in figure 3.6.

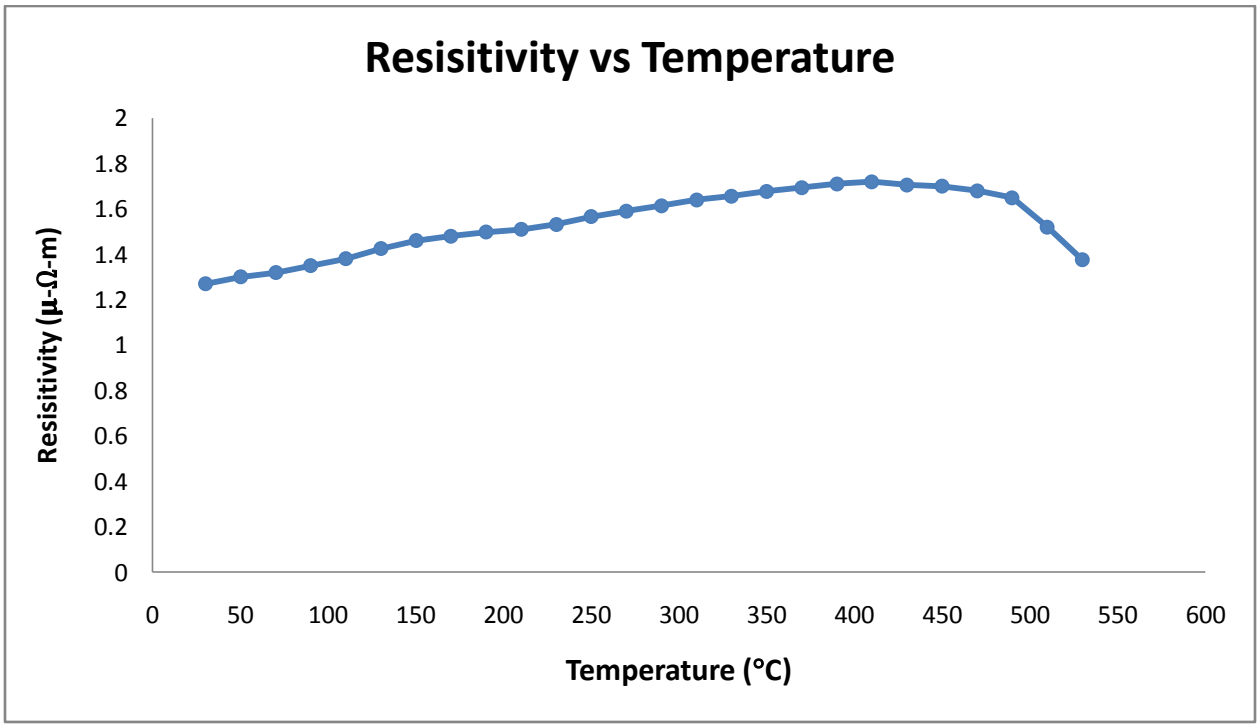

Figure 3.6: Resistivity as a function of Temperature

From the curve we see that the resistivity of the sample does not vary much with the change of the temperature. However, a considerable drop of electrical resistivity is obvious at temperatures above 480^{o}C. This drop is due to the process of crystallization and 480^{o}C can be estimated as the glass transition temperature, T_g of the alloy. In fact

this resistivity drop emphasizes a critical point of each measured alloy. These critical points that could be also detected on the differential scanning calorimetry curves mutually coincide. Due to their insensitivity to temperature variations for temperatures up to 480^{o}C, these metallic glasses are suitable for applications in electronic circuits for which this property is an essential requirement.

3.6 Frequency dependence of relative Permeability

3.6.1 Permeability

Permeability can be defined as the state or quality of being permeable. In other words (Physics / General Physics) a measure of the response of a medium to a magnetic field, expressed as the ratio of the magnetic flux density in the medium to the field strength; measured in henries per metre. In short the ability of a substance to allow another substance to pass through it, especially the ability of a porous rock, sediment, or soil to transmit fluid through pores and cracks.

3.6.2 Relative Permeability

The magnetic constant $\mu_0 = 4\pi \times 10^{-7}$ T m/A is called the permeability of space. The permeability of most materials are very close to μ_0 since most materials will be classified as either paramagnetic or diamagnetic. But in ferromagnetic materials the permeability may be very large and it is convenient to characterize the materials by a relative permeability.

When ferromagnetic materials are used in applications like permeability, the relative permeability gives you an idea of the kind of multiplication of the applied magnetic field that can be achieved by having the ferromagnetic core present. So for an ordinary iron core you might expect a magnification of about 200 compared to the magnetic field produced by the solenoid current with just an air core. This statement has exceptions and limits, since you do reach a saturation magnetization of the iron core quickly, as illustrated in the discussion of permeability.

But in our case, we actually work on the basis of Real and Imaginary part of Permeability with respect to frequency.

3.6.3 Real and Imaginary part of Permeability vs. Frequency

Initial permeability as dependent on frequency of a magnetic material is an important .parameter from the application consideration such as an insulator. Therefore the study of initial permeability has been a subject of great interest from both the theoretical and practical points of view. The optimization of the dynamic properties such as complex permeability in the high frequency range requires a precise knowledge of the magnetization mechanisms involved. The magnetization mechanisms contributing to the complex permeability, $\mu = \mu' - \mu''$, in soft polycrystalline ferrites have been a controversial subject for a long time and remain unsolved satisfactorily. Although it is admitted that two mechanisms are involved in this phenomenon, the domain wall displacement and the spin rotation in the domains.

Complex permeability has been calculated as a function of frequency up to 13 MHz at room temperature for all the samples of the series $\mathbf{Fe_{78}B_{10}Si_{12}}$ ferrites by using the conventional technique based on the determination of the complex impedances of a circuit loaded with toroid shaped sample. The frequency dependent permeability dispersion of ferrites sintered at 1000°C.

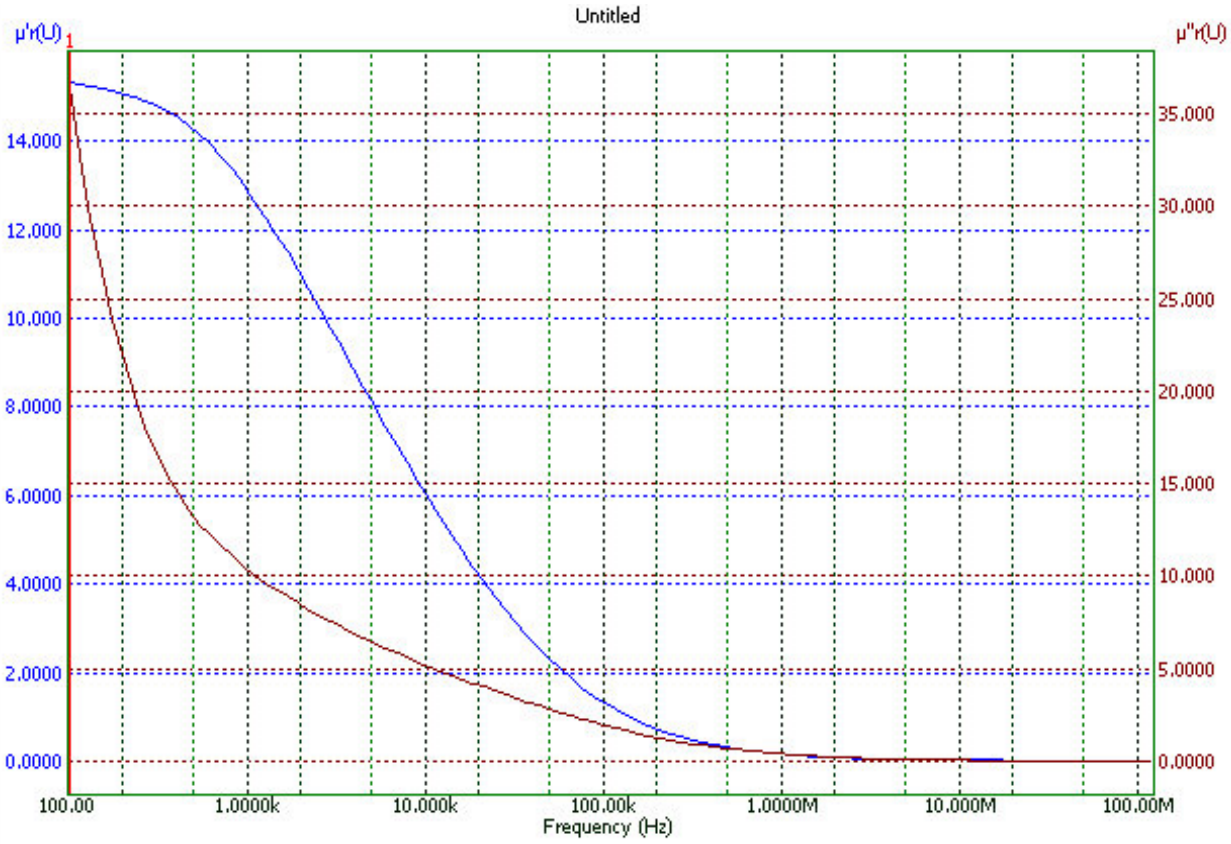

Figure 3.7: Frequency dependence of relative Permeability

In electromagnetism, the auxiliary magnetic field **H** represents how a magnetic field **B** influences the organization of magnetic dipoles in a given medium, including dipole migration and magnetic dipole reorientation. Its relation to permeability is B=μ H.

So it's pretty obvious from the graph that with the increase of frequency i.e. the auxiliary magnetic field increases as if the permeability decreases and it is almost zero at a high frequency of 100MHzIn case of Phase shifting i.e. in case of the complex part of permeability the same phenomena is shown.It (**μ**) becomes almost zero at a frequency of 100MHz.In case of FINEMET the permeability is quite is about 14×10^{5}Tm/A.

3.7 Frequency dependence of relative Permittivity

3.7.1 Permittivity

A property of a dielectric medium that determines the forces that electric charges placed in the medium exert on each other. If two charges of q_1 and q_2 coulombs in free space are separated by a distance r meters, the electrostatic force Fnewtons acting upon each of them is proportional to the product of the charges and inversely proportional to the square of the distance between them. Thus, F is given by Eq. (1),

$$F = q_1 q_2 / 4\pi\varepsilon_0 r^2 \quad (1)$$

where 1/(4&pgr;ε_0) is the constant of proportionality, having the magnitude and dimensions necessary to satisfy Eq. (1). This condition leads to a value for ε_0, termed the permittivity of free space, given by Eq. (2), where

$$\varepsilon_0 = 8.854 \times 10^{-12} \text{ farads/meter} \quad (2)$$

If now the charges are placed in a dielectric medium that is homogeneous and isotropic, the force on each of them is reduced by a factor ε_r, where ε_r is greater than 1. This dimensionless scalar quantity is termed the relative permittivity of the medium, and the product $\varepsilon_0\varepsilon_r$ is termed the absolute permittivity ε of the medium.

A consequence is that if two equal charges of opposite sign are placed on two separate conductors, then the potential difference between the conductors will be reduced by a factor ε_r when the conductors are immersed in a dielectric medium compared to the potential difference when they are in vacuum. Hence a capacitor filled with a dielectric material has a capacitance ε_r times greater than a capacitor with the same electrodes in vacuum would have. Except for exceedingly high applied fields, unlikely normally to be reached, ε_r is independent of the magnitude of the applied electric field for all dielectric materials used in practice, excluding ferroelectrics.

But we examined our sample on the basis of two permittivity categories, they are Real and Imaginary part of permittivity.

3.7.2 Real and Imaginary part of permittivity vs. Frequency

As opposed to the response of a vacuum, the response of normal materials to external fields generally depends on the frequency of the field. This frequency dependence

reflects the fact that a material's polarization does not respond instantaneously to an applied field. The response must always be *causal* (arising after the applied field) which can be represented by a phase difference. For this reason, permittivity is often treated as a complex function of the (angular) frequency of the applied field ω: (since complex numbers allow specification of magnitude and phase).

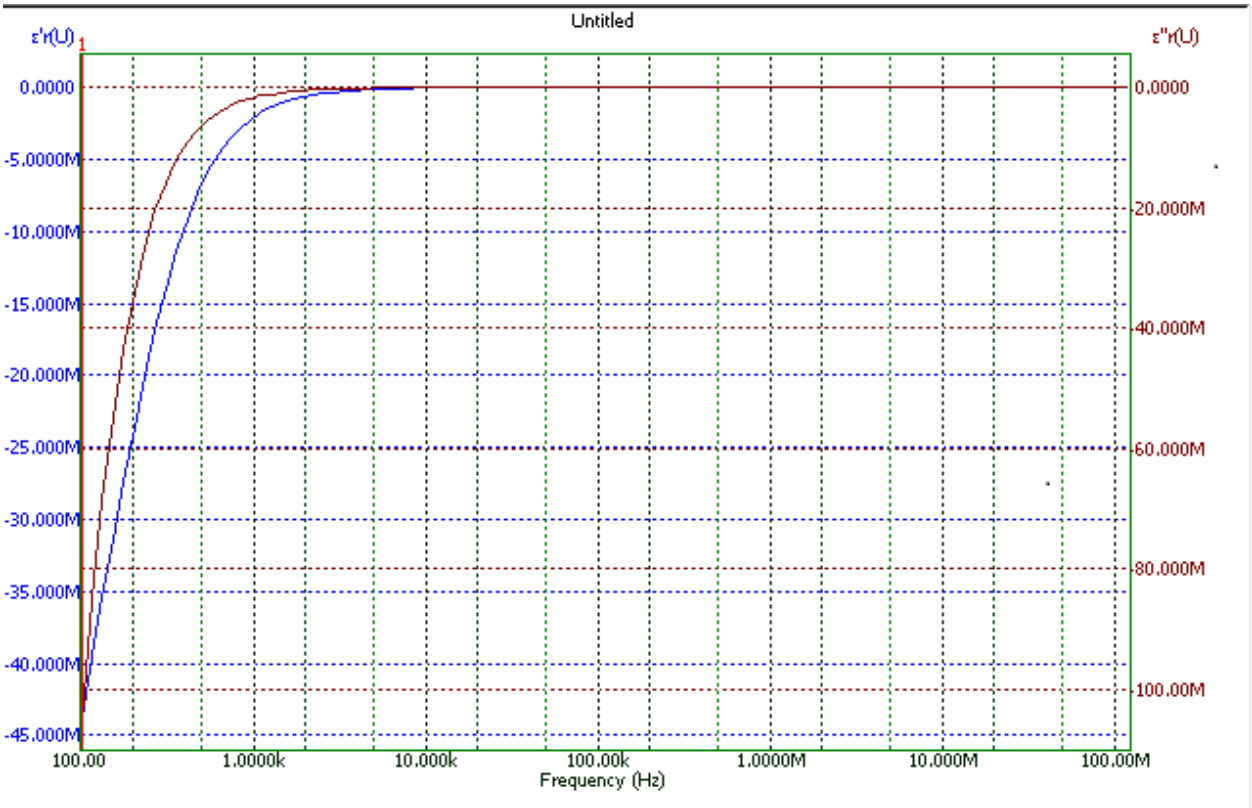

Figure 3.8:Frequency dependence of relative Permittivity

And as a result the effect of real and imaginary part of permittivity is nothing but a certain change in phase.

From the figure we can see that in both real and imaginary cases permittivity becomes almost zero at a frequency of 10kHz having a difference of certain amount of phase shift.

3.8 Quality Factor (Q) and Dissipation factor (D) as a function of Frequency

3.8.1 Quality Factor (Q)

The Q factor or quality factor is a measure of the "quality" of a resonant system. Resonant systems respond to frequencies close to the natural frequency much more strongly than they respond to other frequencies. On a graph of response versus frequency, the bandwidth is defined as the 3 dB change in voltage level besides the center frequency. The definition of the bandwidth as the "full width at half maximum" or FWHM is wrong.

The Q factor is defined as the resonant frequency (center frequency) f_0 divided by the bandwidth Δf or BW:

$$Q = f_o / \Delta f$$

$$\text{Bandwidth BW or } \Delta f = f_2 - f_1$$

wheref_2 is the upper and f_1 the lower cutoff frequency.

In a tuned radio frequency receiver (TRF) the Q factor is:

$$Q = 1/R\sqrt{(LC)}$$

where$R$, L and C are the resistance, inductance and capacitance of the tuned circuit, respectively.

From the expression for the resonant frequency of a tuned circuit,

$$\omega = 1/\sqrt{(LC)}$$

the alternative formulation: $Q = \omega L/R$ can be derived.

In optics, the optical Q factor of a resonant cavity is the ratio of energy stored to energy dissipated in the cavity. If the Q factor of a laser's cavity is abruptly changed, the laser can be induced to emit a pulse of light; this technique is known as Q-switching.

3.8.2 Dissipation Factor (D)

The ratio of the power dissipated in the test material to the power applied. Equal to the tangent of the loss angle, or the cotangent of the phase angle. The dissipation factor can be calculated using:

$$D = \tan \delta = \cot \theta = 1 / (2\pi f R_p C_p)$$

where δ is the loss angle,

θ is the phase angle, f is the frequency,

R_p is the equivalent parallel resistance,

and C_p is the equivalent parallel capacitance.

Quality Factor and dissipation factor are opposite to each other. If QF increases ,DF decreases or vice-versa.

3.8.3 Quality Factor (Q) and Dissipation factor (D) vs. Frequency

We know that the Quality Factor(QF) relates the maximum or peak energy stored to the energy dissipated in the circuit per cycle of oscillation.

Dissipation Factor(DF) means energy dissipated by the circuit in one period of resonance.

Figure 3.9:Quality Factor (Q) and Dissipation factor (D) vs Frequency

Here QF and DF are inversely related to each other as it is clearly visible in the graph.

From the curve it is clearly visible that the sample works as soft magnetic material with low loss at a frequency range of .5k to 100k Hz.

The best response is obtained for the sample where the quality factor of the sample has the height value at the frequency of 10 KHz.

3.9 Frequency dependence of Impedance and Phase angle

3.9.1 Electrical Impedance

Electrical Impedance(Z), is the total opposition that a circuit presents to alternating current. Impedance is measured in ohms and may includeresistance (R),inductive reactance(X_L), and capacitive reactance(X_C). However, the total impedance is not simply the algebraic sum of the resistance, inductive reactance, and capacitive reactance. Since the inductive reactance and capacitive reactance are 90^o out of phase with the resistance and, therefore, their maximum values occur at different times, vector addition must be used to calculate impedance.

The relationship between impedance and its individual components (resistance and inductive reactance) can be represented using a vector as shown in figure (**) The amplitude of the resistance component is shown by a vector along the x-axis and the amplitude of the inductive reactance is shown by a vector along the y-axis. The amplitude of the the impedance is shown by a vector that stretches from zero to a point that represents both the resistance value in the x-direction and the inductive reactance in the y-direction..

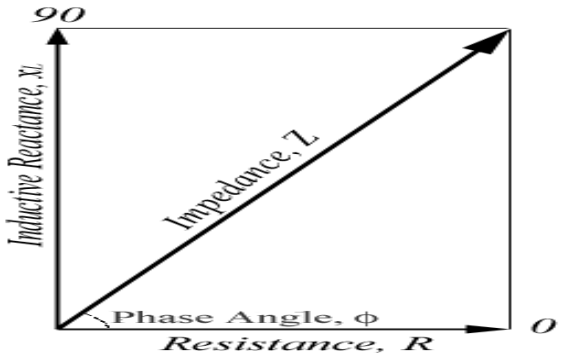

Figure 3.10: Relationship between impedance and its individual components

The impedance in a circuit with resistance and inductive reactance can be calculated using the following equation. If capacitive reactance was present in the circuit, its value would be added to the inductance term before squaring.

$$Z = \sqrt{\left(X_L^2 + R^2\right)}$$

The phase angle of the circuit can also be calculated using some trigonometry. The phase angle is equal to the ratio between the inductance and the resistance in the circuit. With the probes and circuits used in nondestructive testing, capacitance can usually be ignored so only inductive reactance needs to be accounted for in the calculation. The phase angle can be calculated using the equation below. If capacitive reactance was present in the circuit, its value would simply be subtracted from the inductive reactance term.

$$Tan\phi = \frac{X_L}{R} \quad \text{or} \quad \emptyset = \arctan\frac{X_L}{R}$$

3.9.2 Effect of frequency on Impedance

Effect of Frequency on Resistance

Resistance is not affected by frequency.
In an A/C circuit the ratio of voltage to current is called
'Impedance' represented by 'Z' which is a complex quantity.
(V/I) = Z = R + jX.
'R' is the resistance and 'X' is the reactance. jX implies that V & I are at quadrature. X is the sum of 'Inductive' (L) and 'Capacitive' (C) reactance. If 'f' is the frequency
$X = 2\pi f L - [1/2 \pi f C]$.
As you can see X is a function of frequency (and not R that is unaffected by f) whose main effect is to introduce a phase difference between V & I.

Effect of Frequency on Inductive Reactance

In an AC circuit, an inductor produces inductive reactance which causes the current to lag the voltage by 90 degrees. Because the inductor "reacts" to a changing current, it is known as a reactive component. The opposition that an inductor presents to AC is called inductive reactance (X_L). This opposition is caused by the inductor "reacting" to the

changing current of the AC source. Both the inductance and the frequency determine the magnitude of this reactance. This relationship is stated by the formula:

$$X_L = 2\pi fL$$

Where:

X_L = the inductive reactance in ohms
f = the frequency in hertz
L = the inductance in henries
π = 3.1416

As shown in the equation, any increase in frequency, or "f," will cause a corresponding increase of inductive reactance, or "X_L." Therefore, the INDUCTIVE REACTANCE VARIES DIRECTLY WITH THE FREQUENCY. As you can see, the higher the frequency the greater the inductive reactance; the lower the frequency, the less the inductive reactance for a given inductor. This relationship is illustrated in figure 3.11. Increasing values of X_L are plotted in terms of increasing frequency. Starting at the lower left corner with zero frequency, the inductive reactance is zero. As the frequency is increased (reading to the right), the inductive reactance is shown to increase in direct proportion.

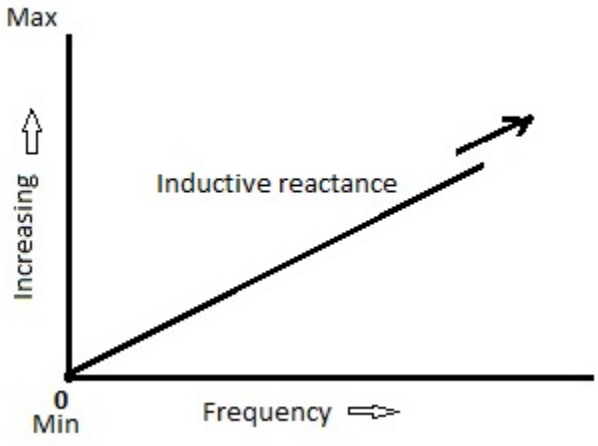

Figure 3.11:Effect of Frequency on Inductive Reactance

Effect of Frequency on Capacitive Reactance

In an AC circuit, a capacitor produces a reactance which causes the current to lead the voltage by 90 degrees. Because the capacitor "reacts" to a changing voltage, it is known as a reactive component. The opposition a capacitor presents to AC is called capacitive

reactance (X_C). The opposition is caused by the capacitor "reacting" to the changing voltage of the AC source. The formula for capacitive reactance is:

$$X_C = \frac{1}{2\pi fC}$$

Where:

X_C = the capacitive reactance in ohms
f = the frequency in hertz
C = the capacitance in farads
π = 3.1416

In contrast to the inductive reactance, this equation indicates that the CAPACITIVE REACTANCE VARIES INVERSELY WITH THE FREQUENCY. When f = 0, X_C is infinite and decreases as frequency increases. That is, the lower the frequency, the greater the capacitive reactance; the higher the frequency, the less the reactance for a given capacitor.

As shown in figure 3.12, the effect of capacitance is opposite to that of inductance. Remember, capacitance causes the current to lead the voltage by 90 degrees, while inductance causes the current to lag the voltage by 90 degrees.

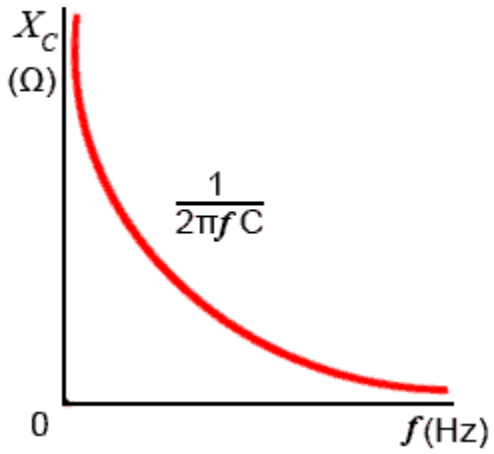

Figure 3.12:Effect of Frequency on Capacitive Reactance

In the expression for inductive reactance, $X_L = 2\pi fL$, and in the expression for capacitive reactance,

$$X_C = \frac{1}{2\pi fC}$$

both contain "f" (frequency). Any change of frequency changes the reactance of the circuit components as already explained. So far, nothing has been said about the effect of frequency on resistance. In an Ohm's law relationship, such as R = E/I no "f" is involved. Thus, for all practical purposes, a change of frequency does not affect the resistance of the circuit. If a 60-hertz AC voltage causes 20 mA of current in a resistive circuit, then the same voltage at 2000 hertz, for example, would still cause 20 mA to flow.

The total opposition to AC is called impedance (Z). Impedance is the combination of inductive reactance (X_L), capacitive reactance (X_C), and resistance (R). When dealing with AC circuits, the impedance is the factor with which you will ultimately be concerned. But, as you have just been shown, the resistance (R) is not affected by frequency. Therefore, the remainder of the discussion of AC circuits will only be concerned with the reactance of inductors and capacitors and will ignore resistance.

AC. Circuits Containing Both Inductive and Capacitive reactance

AC circuits that contain both an inductor and a capacitor have interesting characteristics because of the opposing effects of L and C. X_L and X_C may be treated as reactors which are 180 degrees out of phase. As shown in figure 1-2, the vector for X_L should be plotted above the baseline; vector for X_C, figure 1-3, should be plotted below the baseline. In a series circuit, the effective reactance, or what is termed the RESULTANT REACTANCE, is the difference between the individual reactance. As an equation, the resultant reactance is:

$$X = X_L - X_C$$

3.9.3 Effect of frequency on Phase Angle

When an AC circuit is subjected to a source voltage consisting of a mixture of frequencies, the components in that circuit respond to each constituent frequency in a different way. Any reactive component such as a capacitor or an inductor will simultaneously present a unique amount of impedance to each and every frequency present in a circuit. Thankfully, the analysis of such circuits is made relatively easy by applying the Superposition Theorem, regarding the multiple-frequency source as a set of single-frequency voltage sources connected in series, and analyzing the circuit for one source at a time, summing the results at the end to determine the aggregate total

Because the two voltages across each component are at different frequencies, we cannot consolidate them into a single voltage figure as we could if we were adding together two voltages of different amplitude and/or phase angle at the same frequency.

Complex number notation give us the ability to represent waveform amplitude (polar magnitude) and phase angle (polar angle), but not frequency. But if we increase frequency, then the phase angle starts increasing.

We use Wayne Karr Impedance Analyzer to measure impedance and phase angle with the variation of frequency. We measure the impedance within a range of 100Hz to 100MHz. It reaches a peak just crossing 100kHz and comes down with the increase of frequency. It attains a lower peak near 100MHz which is quite high and again it ascends with the ascending value of frequency. At 100MHz,it reaches a top. So it is clear that the value of phase angle remain low at very high frequencies.

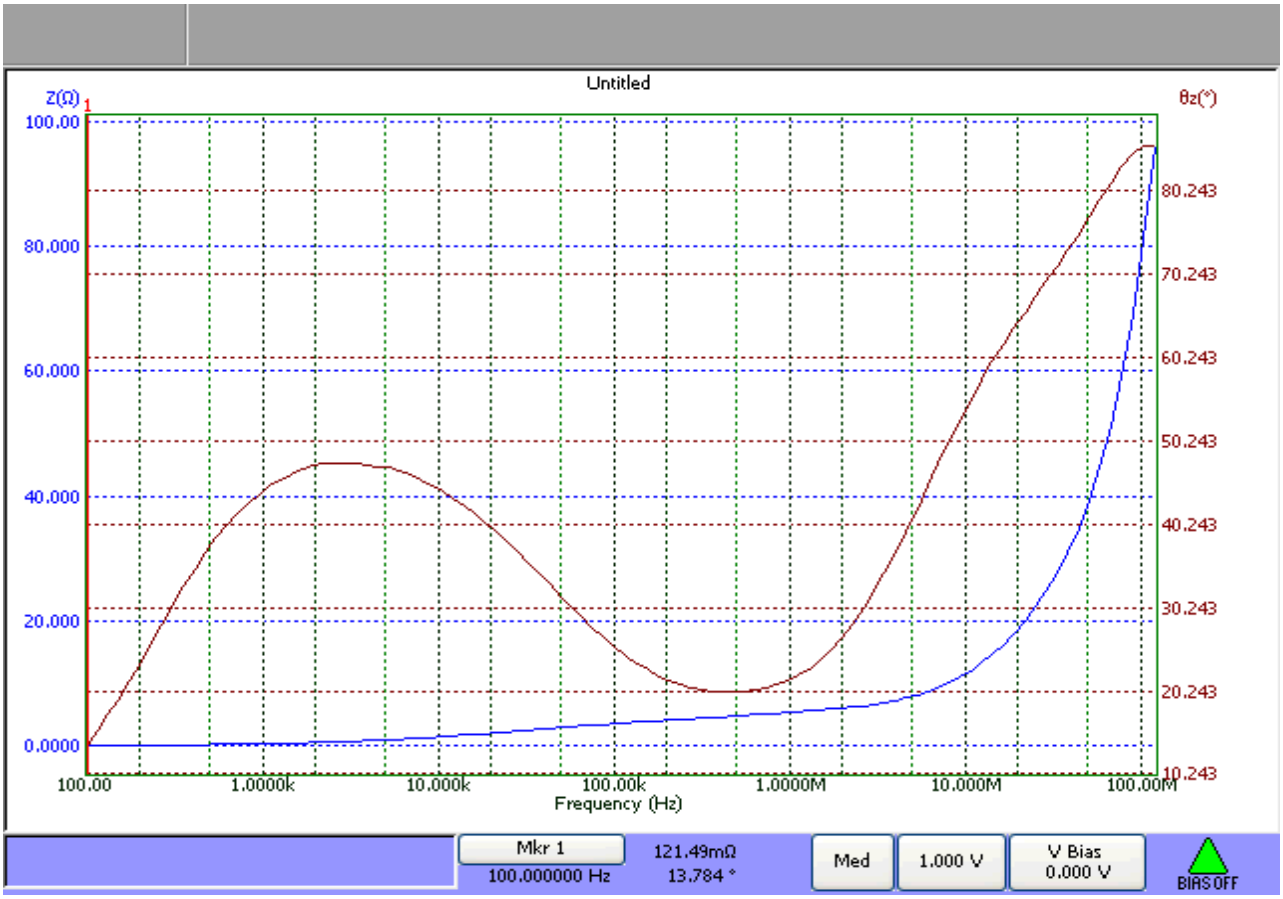

Figure 3.13:Frequency dependence of Impedance And Phase angle

From the curve it is obvious that with the increase in frequency impedance of our sample increases.
It is known to us that the effect frequency on resistance is nothing. But the curve saying impedance is increasing with the frequency. Up to 10MHz impedance increases gradually but after that it increases exponentially. It reaches to about 100Ω from 10 to

100MHz and even further. And this is occurred due to the presence of capacitive and inductive part in the impedance. And it can be said that our material has a wide range of conceding frequency.

Chapter 4

Conclusion

A metglass in the form of ribbon of stoichiometric composition $Fe_{78}B_{10}Si_{12}$ (FINEMET) has been studied for its electrical and magnetic properties. The XRD patterns of all ribbons show no trace of sharp peak which confirms their amorphous nature. The dc electrical resistivity of the sample is estimated to be $1.27\times10^{-6}\Omega m$ at room temperature. The resistivity shows a monotonous and feeble uptrend until the onset of the glass transition temperature T_g (approximately 480^oC) at which the resistivity begins to drop rapidly indicating the segregation of crystalline states. The Magneto Resistance (MR%) which has its origin at the Hall voltage being created in the MUT because of the external applied magnetic field was found to vary from 0-15% a typical value observed in the metallic system. Self-induction caused by an external transducer creates an eddy current hence an AC voltage which is super imposed on the DC response. The oscillating voltage was significant when current through the sample exceeds 0.5A. Permeability of the sample was found to be quite high and by studying frequency dependence of relative Permeability we see that, when the frequency exceeds 10MHz the sample loses its magnetic property as the permeability becomes close to zero. We also found that the permittivity of the sample becomes close to zero over a very small frequency ranging from 5-10 kHz. The best response is obtained at the frequency of 10 KHz for the sample where the quality factor is at its highest value. The changes in impedance were reasonably low with the changes of the frequencies up to 10MHz but afterwards impedance starts to increase rapidly with the increase of the frequency. All together has led to a steadily increasing application of this alloy in magnetic cores for ground fault interrupts, common mode chokes, high frequency transformers and in electrical and magnetic switching devices.

References

[1] Pol.Duwez, J. Vac. Sci. Technol. B, (1983).

[2] H.R Hilzinger, SonderdruckausNTGFachberichten, 76 (1980) 283.

[3] T.R. Anantharaman, Metallic Glasses, Trans Tech Publications (1984) 273.

[4] Cullity, Introduction to Magnetic Materials, Addison Wesley, (1972) 119

[5] Michel Schlenker, Magnetism Fundamentals, Springer (2005) 82

[6] http://www.nims.go.jp/apfim/soft&hard.html

[7] A. Inoue, A. Takeuchi, Mater. Trans. JIM 43 (2002) 1892

[8] W.H. Wang et al, Mat. Sci. Eng. R 44 (2004) 45

[9] Inoue A ,Shen BL, Yavari AR, Greer AL. Mechanical properties of Fe-based bulkglassy alloys in Fe–B–Si–Nb and Fe–Ga–P–C–B–Si systems. J Mater Res20 03;18(6):1487.

[10] Shen J, Chen QJ, Sun JF, Fan HB, Wang G. Exceptionally high glass-forming ability of an FeCoCrMoCBY alloy. ApplPhysLett 20 05;86(15):151907.

[11] Ponnambalam V, Poon SJ, Shiflet GJ, Keppens VM, Taylor R, Petculescu G. Synthesis of iron-based bulk metallic glasses as nonferromagnetic amorphous steel alloys. ApplPhysLett 20 03;83(6):1131–3.

[12] Hess PA , Poon SJ, Shiflet GJ, Dauskardt RH. Indentation fracture toughness of amorphous steel. J Mater Res 20 05;20(4):783–6.

[13] Gu XJ, Poon SJ, Shiflet GJ. Mechanical properties of iron-based bulk metallic glasses. J Mater Res 20 07;22(2):344–51

[14] S.J. Poon et al.: Appl. Phys. Lett. 83, 1131 (2003).

[15] H.S. Chen: J. Non-Cryst. Solids 18, 157 (1975).

[16] J. Schroers and W.L. Johnson: Ductile bulk metallic glass. Phys. Rev. Lett. 93, 255506 (2004).

[17] Lin.C.H et al Solid St. Communs, 29 (1979)

[18] Balanzat, M. Scripta .Met, 14 (1980)

[19] P Petrokowsky, Rev. Sci. lustrum., 34 (1963) 445

[20] S. Kavesh, in "Metallic Glasses \ edited by J J Gilman and H J Leamy, ASM,

Metal Park, 36

[21] T Yamaguchi and K Narita, IEEE Trans. Mag., MAG-13 (1977) 1621

[22] R Glang, "Handbook of Thin Film Technology", edited by L.I Maissel and R

Glang, McGraw Hill, New York (1970)

[23] J L Vossen and W Kern, (eds) "Thin Film Processes", Part II, Academic

Press, New York (1978)

[24] A Brenner, D.E. Couch and E K Williams,./. Res. Nat. Hur. Std, 109 (1950)

[25] A Ali, W A Grant and P J Grundy, Phil. Mag. B 37 (1978) 353

[26] W L Johnson, M Atzmon, M Van Rossum, B.P Dolgin and X L Yeh,

"Proc. 5th Int. Con/, on Rapidly Ouenched Metals", edited by S Steeb and

H WarlimontWurzbue, Germany (1984) 1515

[28] M Von Allmen, "Glassy Metals II", edited by H -J Guntherodt and H Beck

[29] W. Klement et al, Nature 187(1960) 869

[30] D. Turnbull, Trans. AIME (1961) 422

[31] H.S. Chen, D. Turnbull, J. Chem. Phys. 48 (1969)2560

[32] H.S. Chen, Acta Metall. 22(1974)

[33] A.L. Drehman, A.L. Greer, D. Turnbull, Appl. Phys. Lett. 41 (1982) 716

[34] W.H. Kui, A.L. Greer, D. Turnbull, Appl. Phys. Lett. 45 (1984) 615

[35] A. Inoue, T. Zhang, T. Masumoto, Mater. Trans. JIM 30 (1989) 965

[36] A. Inoue, Acta mater. 48 (2000) 279

[37] A. Inoue et al, J. Appl. Phys, 2 (1988)

[38] A. Inoue et al, Mater. Trans. JIM31 (1990)

[39] A. Peker and W.L. Johnson, Appl.Phys.Lett.63 (1993) 2342

[40] A. Inoue, Mater. Trans. JIM 36 (1995) 866

[41] W.L. Johnson, MRS Bull24 (1999) 42

[42] A. Inoue and T. Zhang, Mater. Trans., JIM, 36 (1995) 1184

[43] A. Inoue et al., Mater. Trans., JIM, 37 (1996) 181

[44] A. Inoue et al., Mater. Trans., JIM, 38(1997)179

[45] W.H. Wang et al, Mat. Sci. Eng. R 44 (2004) 45

[46] A. Inoue et al, Mater. Trans. JIM 38(3), (1997) 189